Cytochemistry of defense responses in cassava infected by *Xanthomonas campestris* pv. *manihotis*

K. Kpémoua, B. Boher, M. Nicole, P. Calatayud, and J.P. Geiger

Abstract: Stems of susceptible and resistant cassava plants have been cytologically investigated for their defense reactions to an aggressive strain of *Xanthomonas campestris* pv. *manihotis*. Histochemistry, in conjunction with gold cytochemistry, revealed that in susceptible and resistant plants, phloem and xylem parenchyma cells displayed a wide range of responses that limited the bacterial growth within the infected plants. Lignification and suberization associated with callose deposition were effective mechanisms that reinforced host barriers in the phloem. In the infected xylem, vessels were plugged by a material of pectic and (or) lignin-like origin. Flavonoids have been seen to be incorporated in secondary cell wall coatings. These reactions occurred at a higher intensity in the resistant plants. The number of phoem and xylem cells producing autofluorescent compounds was higher in infected resistant plants than in susceptible plants. Reactions have been observed in the resistant variety only, such as secretion of phenol-like molecules by tyloses and hyperplasic activity of phloem cells that compartmentalized bacterial lysis pockets, which are potent secondary inoculum sources.

Key words: lignin, suberin, callose, phenol, tylose, flavonoid, pectin.

Résumé : Une étude microscopique a été conduite sur les réactions de défense de tiges de variétés de manioc sensibles et résistantes infectées par *Xanthomonas campestris* pv. *manihotis*. Les analyses histochimique et cytochimique ont montré que les cellules parenchymateuses du phloème et du xylème des deux variétés différencient plusieurs réactions susceptibles de limiter la multiplication et la progression de la bactérie dans les tissus. Les synthèses de lignine, de subérine et de callose contribuent au renforcement des barrières constitutives du phloème. Dans le xylème des plantes infectées, les vaisseaux sont obstrués par des dépôts de pectine et de matériel analogue à la lignine, alors que des flavonoïdes ont été détectés dans les tapissements des parois secondaires. Ces réactions apparaissent plus intenses à un même niveau chez la variété résistante; en particulier, le nombre de cellules du phloème et du xylème produisant des composés autofluorescents est statistiquement plus élevé chez les plants résistants infectés que chez les plants sensibles infectés. Par ailleurs, seule la variété résistante est susceptible de différencier des thylles excrétant des composés phénoliques. Chez la même variété, une activité hyperplasique dans le phloème conduit à l'isolement des poches de lyse, sources potentielles d'inoculum secondaire.

Mots clés : lignine, subérine, callose, phénol, thylle, flavonoïde, pectine.

Introduction

Constitutive or induced defense mechanisms contribute to the plant strategy for resistance to microorganisms. Recognition between host plants and microbes results in either incompatibility (Keen 1990) or pathogenesis, during which plant susceptibility varies according to the pathogen aggressiveness (Clarke 1986). Following penetration by phytopathogenic Xanthomonads, plants differentiate a wide range of defense responses. *Xanthomonas* pathovars have been reported to be involved in gene-for-gene interactions (Rudolph 1993) characterized by the hypersensitive reaction (HR). *Xanthomonas campestris* pv. *malvacearum* on cotton (Klement 1982; Essenberg et al. 1992), *X. campestris* pv. *vesicatoria* on tomato (Jones and Scott 1986), and *X. campestris* pv. *campestris* on *Arabidopsis* (Daniels et al. 1991; Lummerzheim et al. 1993) are examples commonly used for studying the race–cultivar interaction.

Resistance of African cassava cultivars (*Manihot esculenta* Crantz) to bacterial blight (CBB) caused by *X. campestris* pv. *manihotis* (XCM) originated from interspecific crossbreeding with *Manihotis glaziovii* and is assumed to be polygenic (Hahn et al. 1980; Perreaux et al. 1978*b*). Race–cultivar combinations have never been evidenced between cassava cultivars and XCM isolates (Boher and Agbobli 1992; Hahn et al. 1980). Rapidity of leaf wound healing, the need for a higher level of inoculum, low vascular colonization by the pathogen, and systemic progression of the pathogen were features demonstrated to be closely associated with cassava resistance to XCM (Boher and Daniel 1985). No variation in mesophyll colonization was observed either in susceptible or resistant cultivars, suggesting that defense genes express in vascular tissues (Boher et al. 1996). The underlying mechanisms of interactions between XCM and cassava have not been analysed at the molecular and cellular levels. Previous studies revealed that resistance was not correlated to leaf phenol content (Teles et al. 1993) and wound healing limited infection in the resistant cultivar (Lambotte and Perreaux 1979; Perreaux et al. 1978*a*).

Received March 11, 1996. Revision received July 8, 1996. Accepted July 12, 1996.

K. Kpémoua, B. Boher,[1] M. Nicole, P. Calatayud, and J.P. Geiger. Laboratoire de phytopathologie, ORSTOM, BP 5045, 34032 Montpellier, France.

[1] Author to whom all correspondence should be addressed.

The present study was conducted to provide cellular evidence of cassava defense responses triggered after infection by XCM. Histo- and cyto-chemical methods, in conjunction with immunocytochemistry, were used for in situ localization of plant molecules involved in cassava resistance to CBB. Emphasis was on phenol localization, reinforcement of constitutive barriers, and vessel occlusions that were shown to occur in vascular tissues. Although similarities in reactions existed between the susceptible and the resistant cultivars tested, we showed that lignin and callose deposits, the occurrence of phenol compounds within the infected vessels associated with suberin, and tylosis may limit disease extension in the resistant plants.

Material and methods

Plant material

In vitro plantlets from the susceptible cultivar Fetonegbodji and the resistant cultivar TMS 91934 were used in this study. They were rendered virus free by thermotherapy and meristem regeneration and then multiplied in culture flasks (Kartha and Gamborg 1975). After transplanting, plants were maintained in pots containing compost. This material was used for artificial infection.

Bacterial strains

The XCM aggressive strain X27 was isolated from naturally infected cassava in Togo. It was grown for 36 h at 30°C on 5% yeast extract – 5% peptone – 5% glucose – 15% agar (Difco, Detroit, Mich.) in Petri dishes. For inoculum preparation, the culture was washed twice in distilled water and collected by centrifugation at 11 000 × *g* for 10 min. The pellet was resuspended in distilled water and photometrically adjusted to 10^8 colony-forming units (CFUs)/mL.

Artificial infection of stems

Eight-week-old plants were infected by puncturing stems at internodes between the first and second fully expanded leaves with a toothpick dipped in the bacterial suspension or in sterile water as a control. Healthy and infected plants were incubated at 27.5 ± 1°C, on a 14 h light : 10 h dark regime (fluorescent, cool white, 40 W) with 85% relative humidity. At 6 days postinoculation, stem fragments were taken 5 and 10 mm above and below the inoculation sites for microscopic observation.

Electron microscopy (EM)

For conventional ultrastructural observations, stem fragments were fixed for 2 h in 2.5% glutaraldehyde buffered with 0.1 M cacodylate buffer (pH 7.2), rinsed in the same buffer, and postfixed for 1 h in 1% osmium tetroxide. Samples were dehydrated in a graded series of alcohol followed by propylene oxide, and then embedded in Epon (TAAB, Aldermarton, England). For immunocytochemistry, samples were fixed for 4 h in 1% glutaraldehyde – 4% paraformaldehyde in the cacodylate buffer, rinsed, and dehydrated in ethanol. Fragments were embedded in LR White (TAAB, Aldermarton, England). Impregnation of stem fragments in resins was processed according to the company recommendation. After thin sectioning, samples were stained and then examined with a JEOL 100EX transmission electron microscope (LPRC, CIRAD, Montpellier, France).

Gold-complexed probes

β-1,4-Glucans were localized using a purified exoglucanase complexed to gold at pH 9 in 0.1 M phospate-buffered saline (PBS) – 0.01 M polyethylene glycol (PEG) (Benhamou et al. 1987). Labeling of sections was performed for 30 min at 25°C on a drop of the gold probe (1/10 dilution) (pH 6.5), followed by washing and staining with lead citrate and uranyl acetate. Specificity of the labeling was assessed by incubating sections with the gold-complexed protein, to which β-1,4-glucan from barley had been added previously.

Cytolocalization of phenol-like compounds was performed with a purified laccase (EC 1.10.3.2) (Geiger et al. 1986) conjugated to colloidal gold. One hundred micrograms of the purified protein was added to stabilize 10 mL of the gold solution at pH 5.02 (Benhamou et al. 1994). Labeling of sections was performed for 30 min at 25°C on a drop of the gold-probe in 0.01% PBS – 0.1 M PEG (pH 6.0). Specificity of labeling was assessed by incubating sections with the gold-complexed laccase previously incubated with an excess of 1% guaïacol, 0.25 M ferulic acid, or 0.15 M chlorogenic acid.

Immunocytochemistry

Polyclonal antibodies raised against β-1,3-glucans (CRB, Cambridge, England) were used for immunolocalization of callose in plants (Northcote et al. 1989). Sections were incubated for 30 min at 25°C on a drop of primary antibodies (1/2000 in 0.1 M PBS (pH 7.2) – 1% bovine serum albumin (BSA) – 0.05% Tween), followed by incubation on fluorescein or gold-labeled goat anti-rabbit antibodies (1/20) (GAR-15, Biocell, Cardiff, England) for fluorescence or EM observations, respectively.

A monoclonal antibody (JIM5) raised against epitopes of unesterified pectin was used to visualize galacturonic acid containing molecules. Immunogold localization of pectin was performed as previously described by Knox et al. (1990). Sections were incubated on a drop of primary antibodies for 2 h at 37°C and then on a drop of a gold-labeled goat anti-rat antibodies (GAT 15, Biocell) for 30 min at 37°C.

Specificity of labeling was assessed through the following control experiments performed on sections from healthy and infected stems: (*i*) incubation with the antiserum previously adsorbed with the corresponding antigen, laminarin, and galacturonic acids, respectively; (*ii*) incubation with preimmune rabbit or rat serum instead of the primary antiserum; and (*iii*) omission of the primary antibody incubation step.

Histochemistry

Cross sections (20–50 μm thick) of fresh infected or healthy stems were cut with a freezing microtome.

Detection of phenolic compounds was performed as described by Daï and Andary (1995). Flavonoids were detected based on their fluorescence and using Neu's reagent; sections were immersed in 1% 2-aminoethyl diphenyl borate in absolute methanol for 2–5 min and examined with an epifluorecence microscope (Diaplan, Leitz, using the Leitz G filter: excitation, 350–460 nm; barrier filter, 515 nm). The vanillin–HCl reagent was used for staining flavan compounds (catechins and condensed tannins); stem sections were immersed for 5 min in 10% w/v vanillin in one volume of absolute ethanol mixed with one volume of concentrated HCl and examined with a light microscope (Diaplan, Leitz). Lignin and suberin were stained with the phloroglucinol–HCl reagent and Sudan IV in alcoholic solution, respectively (Jensen 1962).

Semithin sections (1.5 μm thick) were stained with 0.5% toluidine blue in carbonate buffer (pH 11). Autofluorescence was monitored under UV illumination using the Leitz A2 filter (excitation, 340–380 nm; barrier filter, 430 nm).

Quantitation of cytopathic effects induced by the infection

Comparative analysis of the infection process between susceptible and resistant plants was performed on 10 randomly selected plants for each cultivar. Phenol-producing cells, parenchyma cells associated with vessels, infected vessels, vessels containing tylose, and intercellular bacterial strands were counted on transverse sections made 5 mm away from the infection sites of both cultivars. Data were statistically

Table 1. Quantitation of the infection process 5 mm under the inoculation site, 6 days after inoculation of cassava stems with *Xanthomonas campestris* pv. *manihotis*.

Structural feature	Healthy plants			Infected plants		
	S	R	*P*	S	R	*P*
Phenolic cells[a]						
Cortical parenchyma	36	30	>0.05(ns)	76	48	>0.05(ns)
Phloem	16	28	>0.05(ns)	80	152	<0.01(s)
Xylem	12	16	>0.05(ns)	64	328	<0.01(s)
Medulla	28	40	>0.05(ns)	48	44	>0.05(ns)
Vessel associated-parenchyma cells with dense cytoplasm[b]	16	20	>0.05(ns)	12	340	<0.001(s)
Infected vessels[c]	0	0		22	8	<0.01(s)
Tylose-containing vessels[d]	0	0		14	13	>0.05(ns)
Intercellular bacterial strands[e]	0	0		500	24	<0.001(s)

Note: S, susceptible cultivar; R, resistant cultivar; data are expressed per section as means of 10 observed plants. *P* values are given according to the Mann–Whitney U-test, based on comparison between susceptible versus resistant plants; s, significant; ns, nonsignificant.

[a]Number of parenchyma cells that are stained blue after the use of toluidine blue.

[b]Number of parenchyma cells adjacent to vessels that display a cytoplasm with numerous organelles and no (or small) vacuoles.

[c]Percentage of vessels containing bacteria.

[d]Percentage of vessels that contain tyloses.

[e]Number of bacterial strands in infected stem tissue.

analyzed using the Mann–Whitney U-test at the 0.05 level. The *P* values are given in Table 1.

Results

Histological features of stem tissues from healthy plants

There were no differences in the histology of 2-month-old healthy susceptible and resistant plant stems, including the number of blue-green or dark-blue stained cells after sections treatment with toluidine blue (Table 1) or after autofluorescence observation.

Structural features of XCM-infected cassava

Light microscopy of infected stems revealed that the number of infected xylem vessels and bacterial strands within intercellular spaces of the infected tissues were lower in the resistant cultivar than in the susceptible cultivar (Table 1). Reactions in infected plants occurred both above and below the inoculation sites, but with a higher intensity 5 mm than 10 mm away from these sites. Since differences were similar between the inoculated susceptible and the resistant cultivars at the four levels analyzed, we report here responses observed 5 mm below the infection site and show micrographs of those characterizing resistant plants at this level.

Cytolocalization of phenol compounds

After observation of thick and semithin sections under UV illumination made in healthy tissues, autofluorescence was seen mainly in lignified xylem areas (Fig. 1B) and periphloemic fibers. In infected plants, autofluorescence appeared in phloem and was stronger in xylem tissues of contaminated areas. Intercellular areas filled with bacterial exopolysaccharides were highly autofluorescent. Material that displayed a strong autofluorescence in sieve tubes and xylem vessels (Fig. 1A) was also stained dark blue with the toluidine blue (Fig. 1C). The number of cells that produced phenol-like molecules was higher in xylem and phloem of the resistant than in the susceptible infected plants (Table 1).

Ultrastructural observations of sections from infected stems displayed electron-dense material in phloem and xylem cells. In the infected xylem it was seen coating the vessel secondary cell wall (Fig. 1D). Accumulation of these compounds was found in the vacuoles, cytoplasm, and periplasmic areas of phloem parenchyma cells. They were associated with the endoplasmic reticulum and mitochondria (Fig. 1E).

A fungal laccase conjugated to colloidal gold was used to localize phenol-like molecules in the infected tissues of cassava. In infected plants, labeling was detected over middle lamellae and the primary walls of phloem cells (Fig. 1F). Gold particles were also seen over electron-dense strands occurring within the fibrillar sheath surrounding the pathogen and seldom over bacteria that showed an irregular shape (data not shown). In noninfected plants, labeling was only observed over phenol compounds located within vacuoles of parenchyma cells (data not shown). Incubation of the enzyme–gold conjugate with guaïacol, ferulic acid, or chlorogenic acid prior to section treatment resulted in the presence of a very low labeling (data not shown).

The use of the phloroglucinol–HCl test revealed red-stained material in phloem cells of the infected plants (Fig. 2A). Parenchyma cell walls and material filling sieve tubes were also stained. Similarly, a positive reaction was observed with material that plugged xylem vessels (Fig. 2B). In healthy plants, phloroglucinol-stained material was observed in cell walls of xylem and periphloemic fibers (data not shown). Localization of suberin with Sudan dyes indicated that this aliphatic material was localized within the infected stem phloem late in the infection process. Suberization occurred in cell walls involved in compartmentalization of infected areas (Fig. 2C). In uninoculated plants, suberin was not detected in the stem phloem. Flavonoids were histochemically detected in thin sections after the use of Neu's reagent. Observation under UV

Fig. 1. Phenol localization in infected resistant plants. (A) Fluorescence microscopy of sections in the infected xylem. In vessels, a thin autofluorescent layer is layered on the secondary cell wall (arrows). The middle lamella in intercellular spaces (arrowheads) and the protoxylem cell (*px*) are also autofluorescent. Bar = 15 μm. (B) Fluorescence microscopy of sections in the xylem of healthy plants. The secondary cell wall of the vessel (arrow) is slightly fluorescent. Bar = 10 μm. (C) Light microscopy of semithin sections in the same infected xylem stained with toluidine blue. A dark layer is seen inside the vessels (*vl*) layered over the secondary cell wall (arrows); the middle lamella also stains dark (double arrows). Bar = 10 μm. (D–F) Electron microscopy of phenol-producing cells. (D) An electron-dense layer (arrow) coats the secondary cell wall (*sw*) of an infected vessel (*vl*); *xp*, xylem parenchyma. Bar = 0.25 μm. (E) In phloem parenchyma cells, electron-dense material accumulated within the endoplasmic reticulum (arrows) and the paramural area (double arrow), *m*, mitochondrion; *ml*, middle lamella; *p*, primary cell wall; *v*, vacuole. Bar = 0.6 μm. (F) Cytolocalization of phenol-like molecules by means of a gold-complexed laccase in infected resistant plants. In these phloem cells, gold particles are localized over the middle lamella (arrows) and the primary cell wall (*p*). *m*, mitochondrion; *ml*, middle lamella. Bar = 0.2 μm.

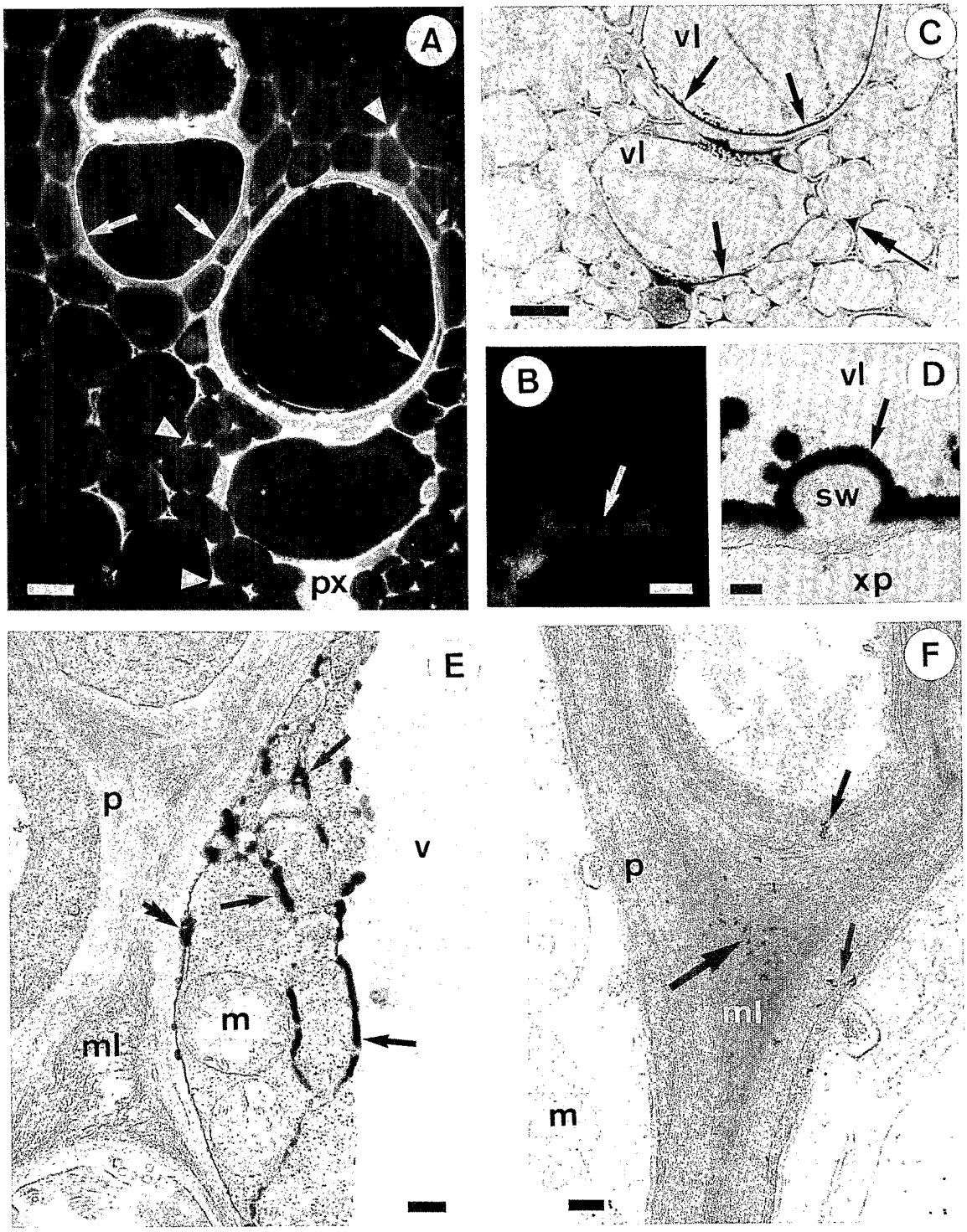

Fig. 2. (A–D) Histochemical localization of phenols in infected resistant plants. (A) Molecules that stain red (arrows) with phloroglucinol–HCl accumulate in the infected phloem within cell walls, sieve tubes, and intercellular spaces. *vl*, vessel. Bar = 20 μm. (B) In infected xylem portions, vessels are plugged with phloroglucinol-positive material (arrows). Bar = 30 μm. (C) Suberized cell walls occur within cambial-like areas as indicated by the red colour of cell walls after the use of Sudan IV (arrows). Bar = 5 μm. (D) Detection of flavonoids using the Neu's reagent. A thin yellow fluorescent layer (arrows) coats the secondary cell walls of two xylem vessels (*vl*). Bar = 7 μm. (E–F) Immunofluorescent detection of callose detection in the resistant cultivar using anti-β-1,3-glucan polyclonal antibodies. Deposits (double arrows) and pads (arrows) of fluorescent material are seen in sieve tubes of the phloem in infected resistant plants (E), while in the noninfected resistant plants, fluorescence occurs at sieve plates only (F, arrows). E, F: bar = 10 μm.

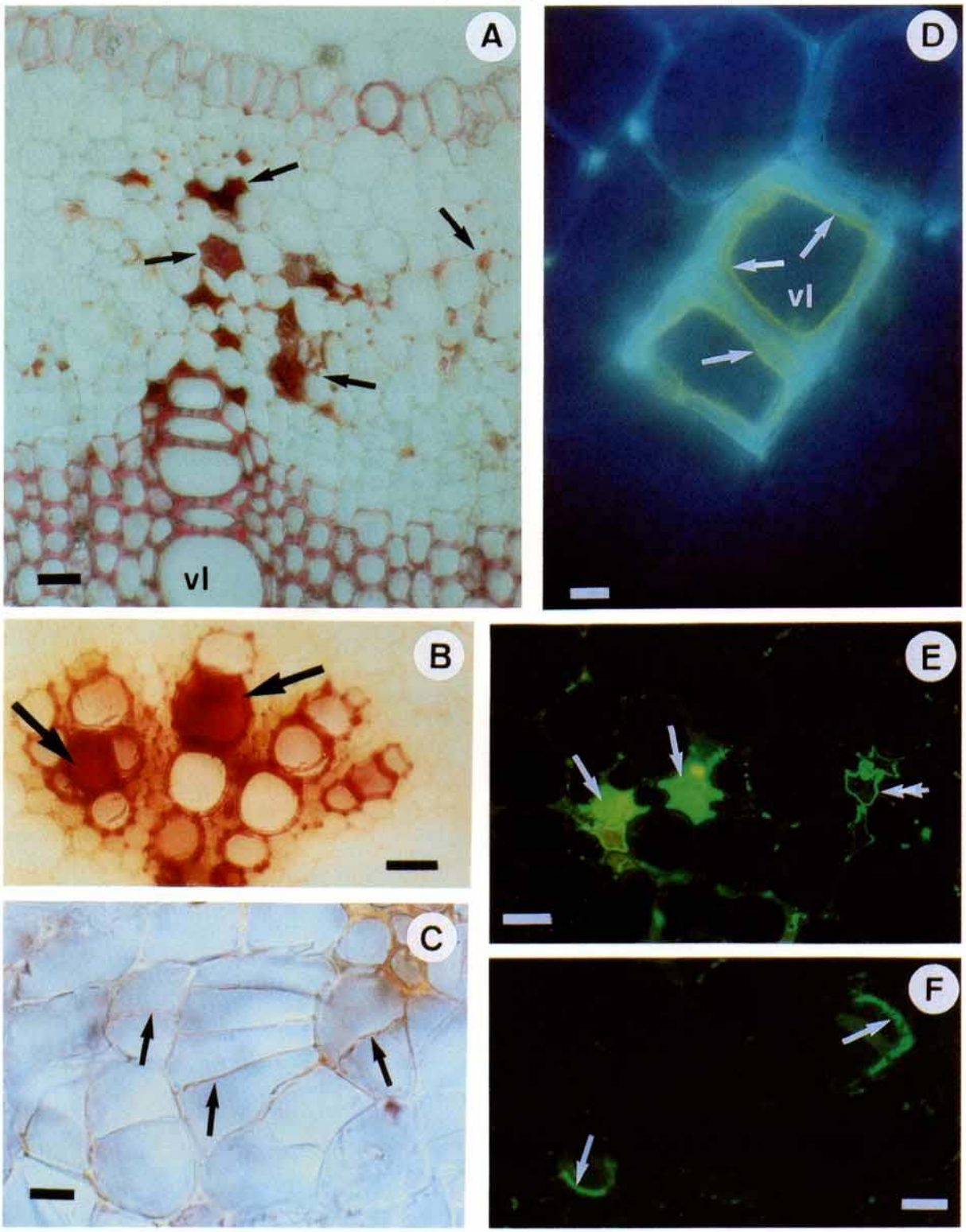

illumination at 365 nm revealed a yellow fluorescence in material coating the secondary cell walls of infected xylem vessels (Fig. 2D). No yellow fluorescence was detected in other portions of infected stem tissues and tissues from healthy plants. The vanillin–HCl treatment showed no difference in the staining of tannin compounds from infected tissues of susceptible and resistant cultivars, as compared with healthy tissues (data not shown).

Cytochemistry of papillae and paramural appositions

Callose, a β-1,3-glucan polymer, was localized using polyclonal antibodies. A strong immunofluorescence was observed in the infected phloem. Pads of callose bordered intercellular spaces and sieve plates and (or) filled sieve tubes (Fig. 2E). In the opposite, a weak immunofluorescence was seen in phloem sieve plates of noninfected plants (Fig. 2F). Immunogold labeling indicated that β-1,3-glucan occurred over portions of the infected phloem. An even distribution of gold particles was seen on material bordering phloem sieve tubes (Fig. 3A) and papillae in intercellular spaces (Fig. 3B). No significant decoration was observed on healthy plant cell walls except over plasmodesmata (Fig. 3E). Pads of heavily labeled material were found to plug plate pores of phloem sieve tube (Fig. 3C); in this case, gold particles were also seen decorating the primary cell wall. Labeling was also detected in parenchyma cells adjacent to vessels. Paramural material of cells in proximity to vessel pits was evenly labeled with the anti-callose antibody as shown in Fig. 3D.

Papillae that were not labeled for β-1,3-glucan detection occurred in intercellular spaces of stem cortical parenchyma. The use of JIM5 anti-pectin monoclonal antibody (not shown) and a gold-complexed exoglucanase for β-1,4-glucan localization (not shown) did not yield any significant labeling of these papillae, while labeling was present on middle lamellae and primary walls in cells close to these papillae.

Ultrastructure and cytochemistry of tylosis

No difference was observed between the infected stems of susceptible and resistant cultivars, where there was an abundant number of tyloses observed in the xylem vessels (Table 1; Figs. 4A and 4B). Portions of tylose middle lamella, as detected by immunolabeling for pectin, were detached from the cell wall (Fig. 4C). These fragments were associated with the vessel secondary cell walls (Fig. 4D), often plugging the cell lumen (data not shown). Amorphous material that could be labeled for β-1,3-glucan (not shown) was observed in close contact with the detached portions of pectin-labeled middle lamella (Fig. 4D).

However, infected resistant and susceptible cultivars differed in the occurrence of striking morphological modifications that were detected in tyloses of the resistant cultivar but not in the susceptible plants. Among tyloses that occluded infected xylem vessels in the resistant plants, some displayed a digit shape (Fig. 5A) and highly electron-dense cytoplasm (Fig. 5B). Vesicles containing opaque material were located close to the plasma membrane; numerous mitochondria and a dense network of endoplasmic reticulum also occurred (Fig. 5C). Portions of tylose wall displayed electron-dense areas, observed nearby the vesicles that contained opaque material (Figs. 5B and 5C). The middle lamella and detached fibrillar fragments adjacent to such wall portions were also electron-dense (Figs. 5B and 6A). Advanced disorganization was characterized by a severe alteration of the cytoplasm and an extreme opacity of the cell wall (Fig. 6A). Numerous collapsed bacteria were detected close to the digit-like tylose containing the electron-dense material (Figs. 5B and 6B), as compared with normal bacteria found in vessels (Fig. 6C).

Hyperplasic activity

In resistant plants only, cell division was observed in parenchyma close to infected areas in both the xylem (Fig. 6D) and the phloem (Fig. 6E). Observation of sections under UV illumination showed a strong autofluorescence in these cambial-like areas (Fig. 6E). Histochemical tests used for lignin or suberin localization revealed the presence of polyphenols and aliphatic compounds associated with newly divided cells (not shown). In the infected susceptible plants, similar cambial-like activity was not detected; in contrast, numerous lysis pockets were seen in the infected phloem and xylem areas (not shown).

Discussion

Successful infection in vascular diseases depends on the plant's capacity to react during colonization of vascular tissues. According to Beckman (1987), few vascular microbes are halted in the mesophyll or cortical tissues by defense responses, although constitutive barriers may slow down the colonization process. When pathogens have reached the xylem elements, systemic invasion of the plant occurs, facilitated by water flow. At this stage, phloem and xylem parenchyma cells only are involved in defense gene expression that will determine the level of plant resistance (Beckman 1987).

The present microscopic study of XCM-infected cassava shows that similar defense responses were elaborated in vascular tissues of both susceptible and resistant plants; however, they were seen with a higher intensity in the resistant cultivar. The lower number of infected vessels and intercellular bacterial strands in the vascular tissues of the infected resistant cultivar as compared with the infected susceptible plants indicates that these defense responses are correlated with reduced disease extension. One of the most conspicuous differences was in the number of phenol-producing cells; while no variation in that number was observed between healthy susceptible and resistant plants, a significant increase in phenolic cells was found first in phloem and later in xylem of the infected resistant cultivar.

It is known that some phenol compounds may have a constitutive role in plant resistance to pathogens while others are synthesized only after elicitation (Mansfield 1983), including newly synthesized lignins, an efficient response that occurs widely in infected plants (Nicholson and Hammerschmidt 1992). Mbaye (1989) reported that 4-methylresorcinol, catechol, quercetin, and ferulic and *p*-coumaric acids extracted from infected cassava have an inhibiting activity on XCM or *X. campestris* pv. *cassavae* growth, although no variation in the total phenol content has been evidenced between susceptible and resistant cultivars (Teles et al. 1993). In contrast, significant differences in flavonoids were detected in sieve tubes and the apoplastic area of the bacterial-resistant cassava attacked by mealybugs (Calatayud et al. 1994). In our study, collapsed bacterial cells that were autofluorescent or labeled by a

Fig. 3. Cytochemistry of papillae and paramural deposits in infected resistant plants: immunogold localization of callose using anti-β-1,3-glucan polyclonal antibodies. (A) Gold-labeled material (arrows) coats the cell wall of a degraded phloem sieve tube (*st*). *cc*, companion cell; *p*, primary cell wall. Bar = 0.3 μm. (B) A papilla located in the intercellular space (*is*) in the infected phloem is evenly labeled (arrows); no significant labeling is seen over the primary cell walls (*p*) and middle lamella (*ml*) Bar = 0.3 μm. (C) Numerous gold particles occur over a pad of callose (arrows) that plugs pores (double arrows) of a sieve plate (*st*); labeling is also present over the primary cell wall (*p*). Bar = 0.5 μm. (D) Deposits of labeled material (arrows) are found in the paramural area of a parenchyma cell (*cc*) adjacent to an infected vessel (*sw*, secondary cell wall). Bar = 0.3 μm. (E) Gold-labeled material (arrows) is seen over a plasmodesmatal area between two phloem cells of a noninfected plant. *p*, primary wall; *m*, mitochondrion. Bar = 0.25 μm.

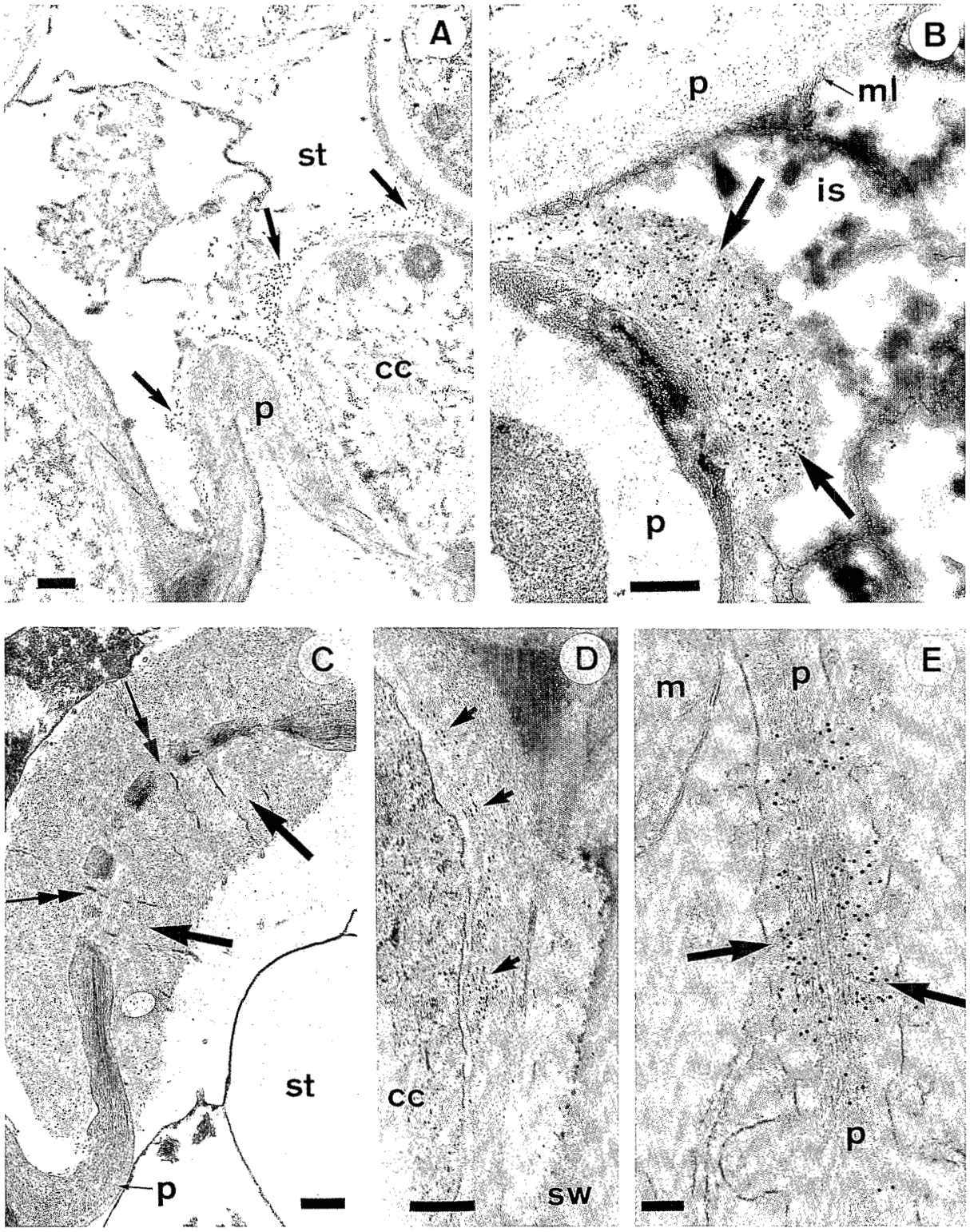

Fig. 4. Light and electron microscopy of tyloses in vessels of infected resistant plants. (A) Semithin section stained with toluidine blue. This portion of infected stem xylem displays several vessels that are plugged by tyloses (*t*). Parenchyma cells adjacent to vessels are dark stained (arrows). *cv*, contaminated vessel. Bar = 20 μm. (B–D) Ultrastructure and cytochemistry of tyloses. (B) Ultrastructure of several tyloses (*t*1, *t*2, *t*3, and *t*4) plugging a vessel lumen in the xylem of the susceptible cultivar. Unidentified material (arrows) between the secondary wall (*sw*) and tylose cell wall. Bar = 2 μm. (C) Gold labeling of pectin using JIM5 monoclonal antibody indicates that fragments of middle lamella (arrows) detach from the tyloses and occur within the infected vessel (*vl*). Bar = 0.25 μm. (D) Material labeled with JIM anti-pectin monoclonal antibody (arrows) is seen between the tylose (*t*) cell wall (*p*) and the vessel secondary cell wall (*sw*); amorphous material (double arrows) and electron-dense droplets (arrowheads) are associated with pectin-like molecules. Bar = 0.25 μm.

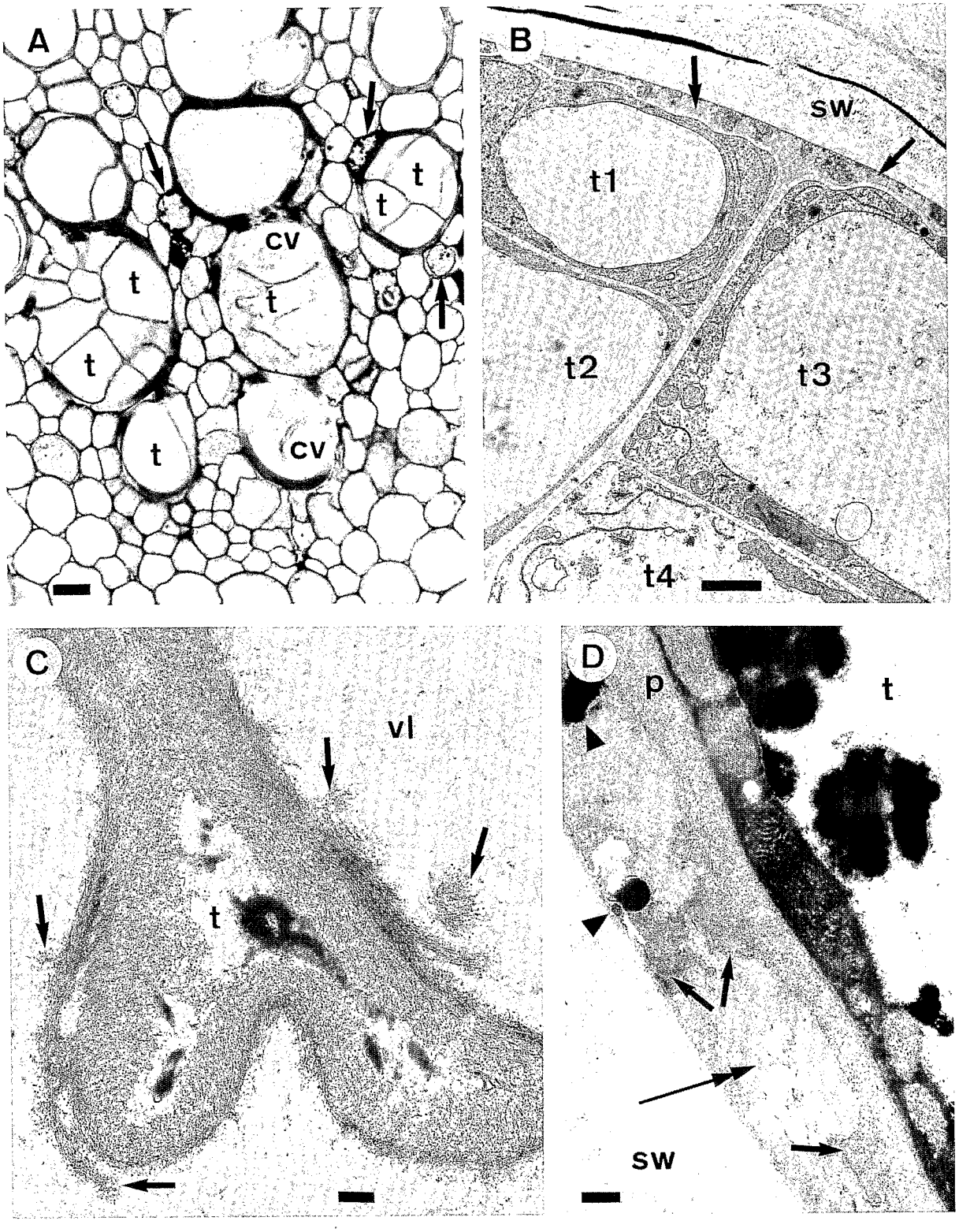

Fig. 5. Ultrastructure of tyloses in vessels of infected resistant plants. (A) The tylose in the infected vessel (*vl*) has a digited shape showing an electron-dense cytoplasm and middle lamella (*ml*). Numerous bacteria (*b*) surrounded by a fibrillar sheath (*s*) are located around the tylose. Note detached fragments from the tylosis middle lamella (arrows). *sw*, secondary cell wall. Bar = 2 μm. (B) Vesicles containing opaque material are seen in the electron-dense cytoplasm of this digited tylose. Cell wall areas are also seen as electron dense (arrowheads). Bacteria displaying irregular shape are located in the vicinity of the tylose (arrows), while others show a normal shape (double arrows). *vl*, vessel. Bar = 1 μm. (C) Enlargement of Fig. 5B showing cytoplasmic vesicles that contain electron-dense molecules (double arrows). The tylosis (*t*), cell wall (*p*), and middle lamella (*ml*) also display areas with intense opacity (arrows). Numerous mitochondria (*m*) and ribosomes, and a dense network of endoplasmic reticulum (*er*) are located close to the electron-dense vesicles. Bar = 0.2 μm.

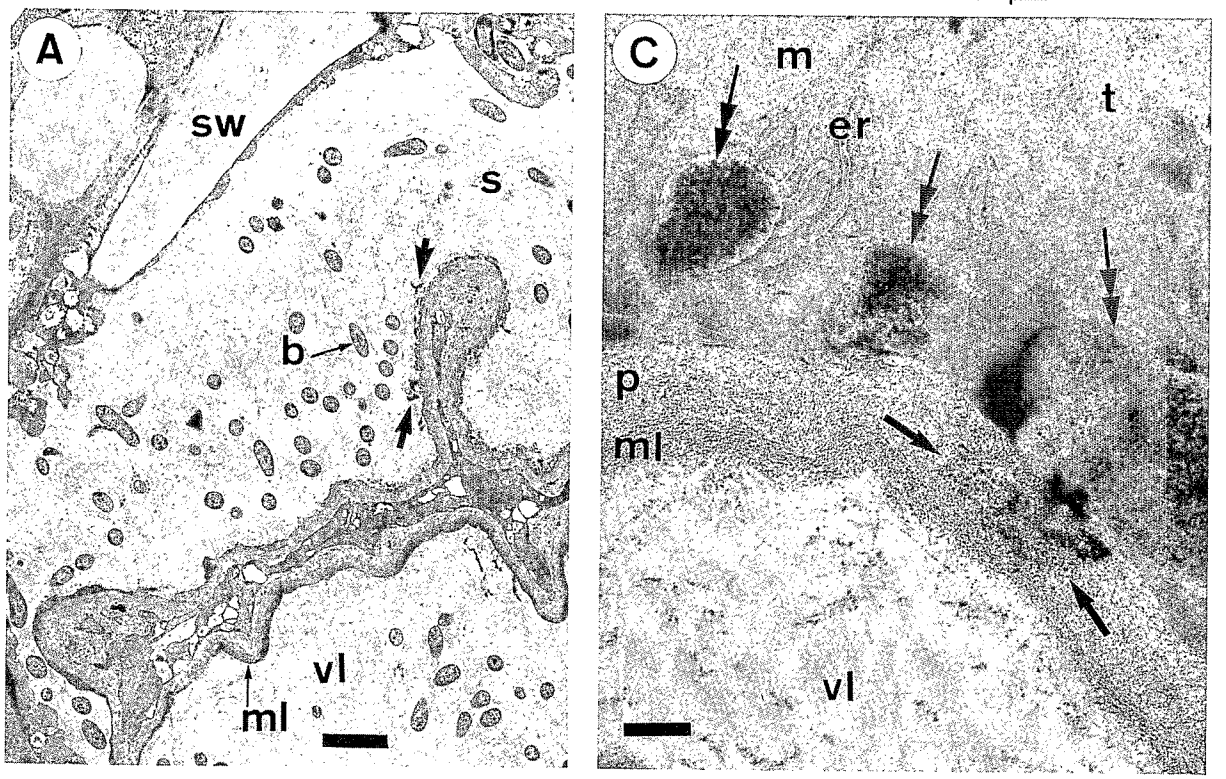

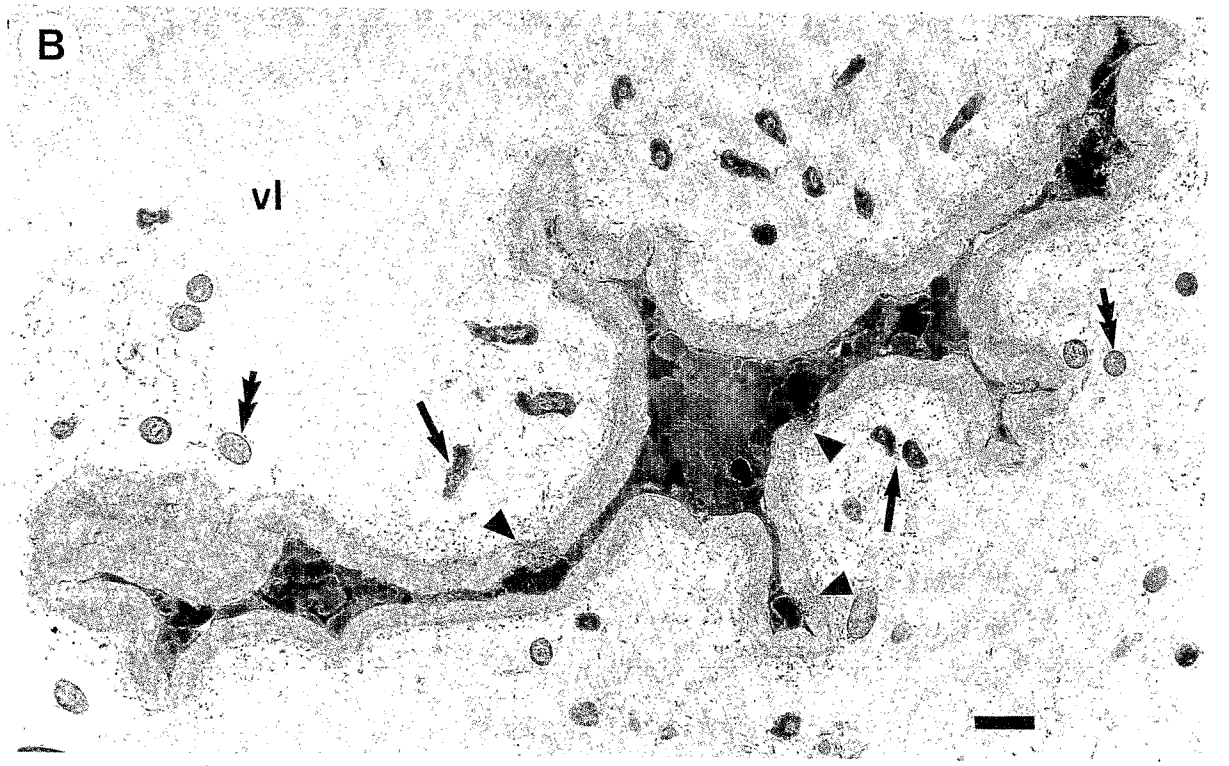

Fig. 6. (A–C) Electron microscopy of tylosis in vessels of infected resistant plants. (A) Necrotic tyloses (*t*) with intense opacity of the cell wall (*p*) and middle lamella. Fibrils of the cell wall are decorated with electron-dense droplets (arrows) both inside and outside the tylosis, the cytoplasm of which appears to be severely altered (*vl*, vessel). Bar = 0.1 μm. (B–C) Close to the digited tylosis, collapsed bacterial cells are seen (B) in association with bacteria showing a regular shape (C). B, C: bar = 0.2 μm. (D–E) Light microscopy of cambial zones in stems of infected resistant plants. (D) Semithin section stained with toluidine blue showing cambial cells (arrows) close to an infected xylem area. A tylose is seen within a vessel (double arrow) close to two contaminated vessels (*cv*). Bar = 20 μm. (E) Observation of a thick section showing autofluorescence of a cambial zone (arrows) close to the infected phloem (*ph*). Autofluorescence of cell walls indicates the presence of phenol-like compounds. *pf*, phloem fibers. Bar = 20 μm.

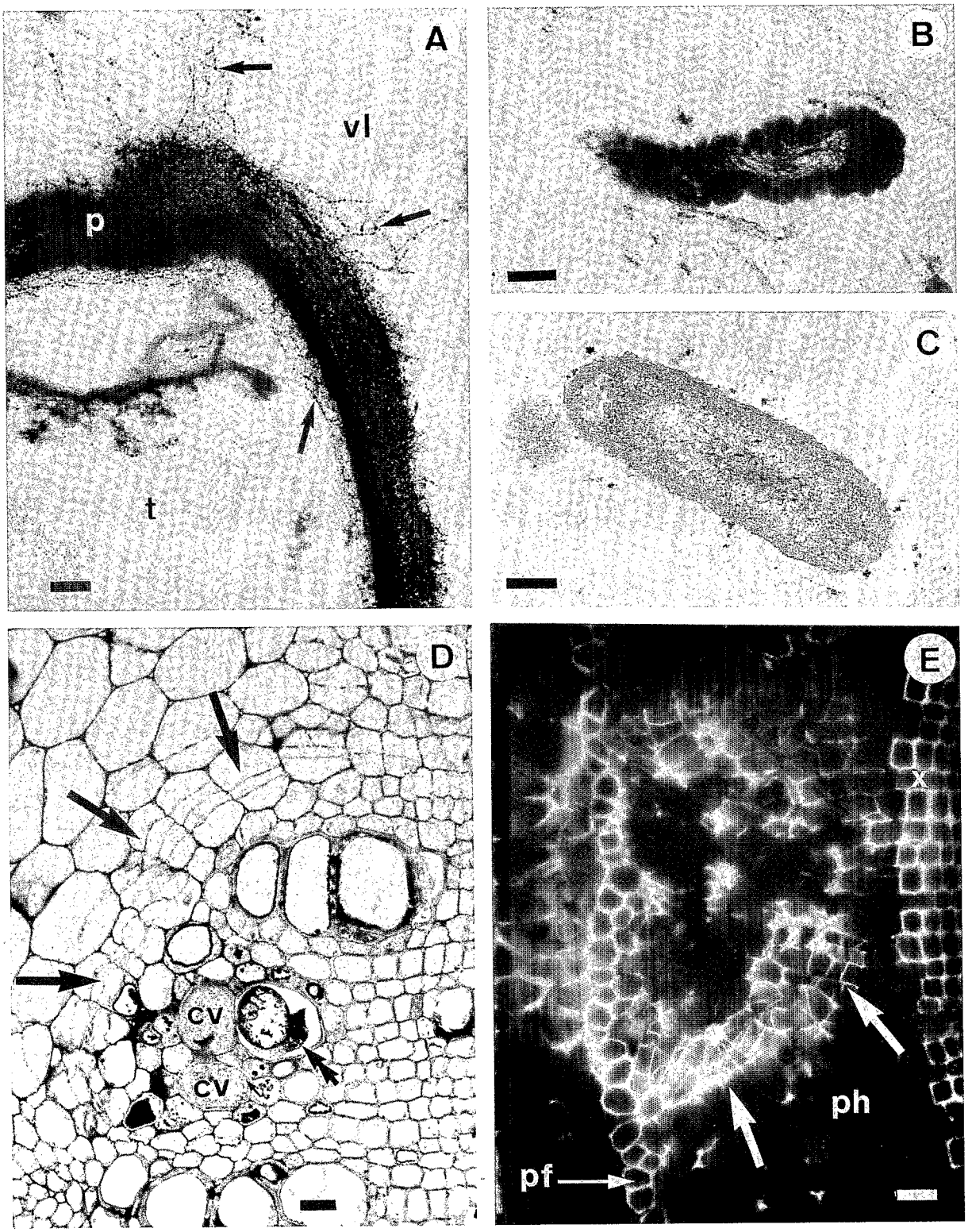

laccase–gold complex were seen in phenol-containing areas, suggesting that these compounds may have a bactericidal effect in planta. Several lines of experimental evidence have revealed bactericidal activity of phenolics in *Xanthomonad*-infected plants such as rice (Horino and Kaku 1989; Reimers and Leach 1991), *Pelargonium* (Wainwright and Nelson 1972), cotton (Jalali et al. 1976), and cabbage (Nmasivayam et al. 1971). Flavonoids and catechic compounds inhibit growth of *X. campestris* pv. *glycines* (Holliday and Keen 1982), *X. campestris* pv. *vesicatoria* (Wymann and Van Etten 1978), *X. campestris* pv. *pelargonii*, and *X. campestris* pv. *malvacearum* (Jalali et al. 1976; Daï et al. 1996). In our model, flavonoids were histochemically detected only within infected vessels in the coating material. Although additional layers within xylem vessels have been reported during interactions between plants and pathogenic bacteria (Horino and Kaku 1989; Molenhauer and Hopkins 1976; Vasse et al. 1995; Wallis and Truter 1978), the occurrence of flavonoid compounds in vessel coating layers was not mentioned.

That phenols were in XCM fibrillar polysaccharidic sheath (xanthan) was cytochemically confirmed by UV illumination and the labeling pattern observed after incubation of sections with a gold-complexed laccase. In light of the detection of laccase-bound molecules at a distance from phenol-producing sites, it is logical to assume that plant phenols may diffuse within bacterial exopolysaccharides.

In addition to accumulation of unidentified phenolics, lignins were also localized in walls of infected cassava phloem and cortical cells, preventing the formation of bacterial lysis pockets, which are potent secondary inoculum sources. The lignin deposits within middle lamellae likely contribute to halting the extension of bacterial intercellular strands, as suggested by the decrease in the number of colonized intercellular spaces of resistant plants. Incorporation of lignin in phloem pectic polymers may inhibit XCM pectic enzymes involved in pectin degradation (Boher et al. 1995). A similar conclusion was drawn by Lyon and McGill (1989) and Lyon et al. (1992) in the case of potatoes infected by *Erwinia carotovora*. Lignin deposits may also stop nutrient diffusion from sieve tube cell walls towards intercellular spaces where bacteria grow. Suberin, a fatty-acid-esterified phenylpropanoid polymer (Kolattukudy et al. 1994), might also be present in the infected phloem and protoxylem cells of resistant cassava. Although evidenced late during pathogenesis, sudan staining was always associated with cell hyperplasia likely to compartmentalize infected areas and to prevent the formation of lysis pockets as previously reported (Lemattre 1963; Lambotte and Perreaux 1979; Wainwright and Nelson 1972).

During invasion of the cassava vascular tissues, amorphous material occurred within intercellular and paramural areas of phloem cells, as well as in infected vessels. Immunogold labeling of β-1,3-glucan revealed that these wall appositions were enriched with callose. Deposition of callose has been widely documented in pathogenic interactions (Benhamou et al. 1994; Daayf et al. 1996), including relationships between plants and bacteria (Bestwick et al. 1995; Boher et al. 1996). In XCM-resistant cassava interactions, the association of lignin and suberin deposits with callose strongly contributes to the reinforcement of host cell walls and to limitation of bacterial development in the infected phloem, similarly to the accumulation of cellulose, pectin, and unknown compounds found in paramural papillae (Boher et al. 1996).

One of the common responses to vascular microbes is the differentiation of tyloses that partially or completely occlude xylem vessels (Beckman 1987). Tyloses with a globular shape result from outgrowths of vessel-associated parenchyma cells that balloon through pit cavities into adjacent tracheary elements. They contribute to stopping the pathogen transportation within xylem vessels (Beckman and Talboys 1981; Bell 1992; Ouellette and Rioux 1992; VanderMolen et al. 1987). Sometimes, tyloses become lignified or suberized, thus increasing the cell wall rigidity (Rioux et al. 1995). The occurrence of tylose formation in bacterial diseases is poorly documented. In Pierce's disease, Mollenhauer and Hopkins (1976) demonstrated that the number of tyloses is higher in tolerant than in susceptible plants. Similarly, Grimault et al. (1993) pointed out the role of these structures in resistant tomato plants attacked by *Pseudomonas solanacearum*. Wallis and Truter (1978) demonstrated that bacteria migrated into tomato tyloses before being liberated within vessels. In contrast, infection by *X. campestris* pv. *pelargonii* did not induce significant differences in the production of tylosis between susceptible and resistant *Pelargonium* plants (Wainwright and Nelson 1972). Accordingly, the present data clearly indicate that tyloses differentiated in the infected cassava cultivar were not quantitatively involved in resistance to XCM.

The contribution of tyloses to cassava defense reactions deals with production of occluding material in xylem vessels of the host plant. Detached wall fragments accumulated in vessel lumina close to the secondary cell walls. Previous works were reported on gels and gums that plug infected vessels in responses to vascular pathogens (Beckman 1987; Moreau et al. 1978; Tsuno and Wakimoto 1989; VanderMolen et al. 1977). Although the pectic nature of gels and gums has been suspected after staining with ruthenium red, in the present study we proved immunologically for the first time that such occluding material contains pectic elements. We also characterized the presence of β-1,3-glucan and lignin-like molecules within this vessel-plugging material (Boher et al. 1995) that could be excreted either by tyloses or other vessel-associated parenchyma cells. This observation is in accordance with works of Bretschneider et al. (1989), who stained callose deposits with the sirofluor dye in cabbage vessels invaded by *X. campestris* pv. *campestris*.

In infected resistant cassava plants, ultrastructural observations showed strong modifications of induced tyloses that displayed a digit-like shape during pathogenesis. The collapsing process of tyloses is associated with an apparent increase in the number of organelles (endoplasmic reticulum, Golgi apparatus, and mitochondria) and the apparition of numerous vesicles. Those vesicles appeared to secrete electron-dense compounds in paramural areas first, and in the vessel lumina second, throughout the tylose cell wall. The affinity of these molecules for osmium tetroxide and toluidine blue, as well as their autofluorescence when sections were observed under UV illumination, strongly suggest that these secreted compounds are of phenolic origin. The presence of dead bacterial cells close to the excreting sites or in the vicinity of such tylose indicates that these phenol-like molecules may have a bactericidal effect. The intense cytoplasmic activity of such tyloses should be related to the dense cytoplasm of vessel contact

parenchyma cells where tyloses originate from. In light of these observations, we can assume that in resistant cassava plants infected by XCM, degradation of tyloses is associated with the secretion of phenolics that may be locally toxic for the pathogen. The possible role of these tyloses in plant resistance remains, however, to be evaluated. To our knowledge, such a mechanism has never been described before in vascular diseases.

In conclusion, the present ultrastructural and cytochemical study on cassava revealed that a wide range of defense mechanisms are activated both in susceptible and resistant cultivars during interactions with XCM. Our observations indicate that parenchyma cells in phloem vessels or adjacent to xylem vessels play an important role in the defense strategy of resistant plants. Colonization of stem phloem by the pathogen triggers callose and phenol synthesis, including lignin, which we consider as early responses regarding the infection process in cassava. The second line of defense to XCM invasion occurs in xylem, where several reactions result in intense changes in the metabolism of parenchyma cells adjacent to vessels. Reinforcement of cell walls and deposition of paramural material are associated with incorporation of lignin, flavonoids, and polysaccharides such as callose, pectin, and cellulose. In parallel, bactericidal phenol-like molecules may be secreted by tyloses within infected vessels in association with accumulation of pectin and callose. Late in the infection, hyperplasia of phloem or xylem cells associated with lignification and suberization of cell walls is a defense response that may lead to compartmentalization of bacterial lysis pockets. These defense responses could constitute a selective advantage for resistant cassava plants to limit or stop bacterial blight extension.

References

Beckman, C.H. (*Editor*). 1987. The nature of wilt diseases of plants. APS Press, St. Paul, Minn.

Beckman, C.H., and Talboys, P.W. 1981. Anatomy of resistance. *In* Fungal wilt diseases of plants. *Edited by* M.E. Mace, A.A. Bell, and C.H. Beckman. Academic Press, New York. pp. 487–521.

Bell, A. A. 1992. *Verticillium* wilt. *In* Cotton diseases. *Edited by* R.J. Hillocks. CAB International, Wallingford, U.K. pp. 87–126.

Benhamou, N., Chamberland, H., Ouellette, G.B., and Pauzé, F.J. 1987. Ultrastructural localization of β-1,4-glucans in two pathogenic fungi and their host tissues by means of an exoglucanase-gold complex. Can. J. Microbiol. **33**: 405–417.

Benhamou, N., Lafontaire, P.J., and Nicole, M. 1994. Seed treatment with chitosan induces systemic resistance to *Fusarium* crown, and root rot in tomato plants. Phytopathology, **45**: 1432–1444.

Bestwick, C.S., Bennett, M.H., and Mansfield, J.W. 1995. *Hrp* mutants of *Pseudomonas syringae* pv. *phaseolicola* induces cell wall alterations but not membrane damage leading to the hypersensitive reaction in lettuce. Plant Physiol. **108**: 503–516.

Boher, B., and Agbobli, C.A. 1992. La bactériose vasculaire du manioc au Togo : caractérisation du parasite, répartition géographique et sensibilité variétale. Agron. Trop. **46**: 131–136.

Boher, B., and Daniel, J.F. 1985. Recherche des sites d'expression de la tolérance vis-à-vis de *Xanthomonas campestris* pathovar *manihotis* (Arthaud-Berthet) Starr chez certains cultivars de manioc (*Manihot esculenta* Crantz). Agronomie, **5**: 677–683.

Boher, B., Kpémoua, K., Nicole, M., Luisetti, J., and Geiger, J.P. 1995. Ultrastructure of interactions between cassava, and *Xanthomonas campestris* pv. *manihotis*: cytochemistry of cellulose, and pectin degradation in a susceptible cultivar. Phytopathology, **85**: 777–788.

Boher, B., Brown, I., Nicole, M., Kpémoua, K., Bonas, U., Geiger, J.P. and Mansfield, J. 1996. Histology and cytochemistry of interactions between plants and *Xanthomonas*. *In* Histology, ultrastructure and molecular cytology of plant–microorganism interactions. *Edited by* M. Nicole, and V. Gianinazi-Pearson. Kluwer Academic publishers, Dordrecht, the Netherlands. pp. 193–210.

Bretschneider, K.E., Gonella, M.P., and Robeson, D.J. 1989. A comparative light and electron microscopical study of compatible and incompatible interactions between *Xanthomonas campestris* pv. *campestris* and cabbage (*Brassica oleracea*). Physiol. Mol. Plant Pathol. **34**: 285–297.

Calatayud, P.A., Rahbe, Y., Delobel, B., Khuong-Huu, F., Tertuliano, M., and Le Rü, B. 1994. Influence of secondary compounds in the phloem sap of cassava on expression of antibiosis towards the mealybug *Phenacoccus manihoti*. Entomol. Exp. Appl. **72**: 47–57.

Clarke, D.D. 1986. Tolerance of parasites and disease in plants and its significance in host–parasite interactions. Adv. Plant Pathol. **5**: 161–197.

Daayf, F., Nicole, M., Boher B., Pando, A., and Geiger, J.P. 1996. Early defense reactions of cotton roots to *Verticillium dahliae*. Eur. J. Plant Pathol. In press.

Daï, G.H., and Andary, C. 1995. Comparison of histochemical reactions of two types of grapevine tissue (plants in the glasshouse plantlets *in vitro*) to infection by *Plasmopara viticola*. Phytopathology, **85**: 149–154.

Daï, G.H., Nicole, M., Andary, C., Martinez, C., Bresson, E., Boher, B., Daniel, J. F. and Geiger, J. P. 1996. Histochemistry and ultrastructure of flavonoids that accumulate during an incompatible interaction between *Xanthomonas campestris* pv *malvacearum* (Race 18) and cotton. Physiol. Mol. Plant Pathol. In press.

Daniels, M.J., Barber, C.E., Dow, J.M., Cough, C.L., Osbourn A.E., and Tang, J. L. 1991. Molecular genetic dissection of pathogenicity of *Xanthomonas*. *In* Biochemistry and molecular biology of plant–pathogen interactions. *Edited by* C.J. Smith. Oxford Science for Publications, Oxford, U.K. pp. 152–162.

Essenberg, M., Pierce, M.L., Hamilton, B., Cover, E.C., Scholes, V.E., and Richardson, P.E. 1992. Development of fluorescent, hypersensitively necrotic cells containing phytolalexins adjacent to colonies of *Xanthomonas campestris* pv. *malvacearum* in cotton leaves. Physiol. Mol. Plant Pathol. **41**: 85–99.

Geiger, J.P., Rio, B., Nandris, D., and Nicole, M. 1986. Laccases of *Rigidoporus lignosus* and *Phellinus noxius*. I. Purification, and some physico-chemical properties. Appl. Biochem. Biotechnol. **12**: 121–133.

Grimault, V., Gelie, B., Lemattre, M., Prior, P., and Schmit, J. 1993. Comparative histology of resistant, and susceptible tomato cultivars infected by *Pseudomonas solanacearum*. Physiol. Mol. Plant Pathol. **44**: 105–123.

Hahn, S.K., Howland, A.K., and Terry, E.R. 1980. Correlated resistance of cassava to mosaic and bacterial blight diseases. Euphytica, **29**: 305–311.

Holliday, M.J., and Keen, N. 1982. The role of phytoalexins in the resistance of soybean leaves to bacteria: effect of glyphosate on glyceollin accumulation. Phytopathology, **72**: 1470–1474.

Horino, O., and Kaku, H. 1989. Defense mechanisms of rice against bacterial blight caused by *Xanthomonas campestris* pv. *oryzae*, the bacterial blight of rice. *In* Proceedings of the International Workshop, March 1988. International Rice Research Institute, Manila, Philippines. pp. 14–18.

Jalali, B.L., Singh, G., and Groveer, R.K. 1976. Role of phenolics in bacterial blight resistance in cotton. Acta Phytopathol. Acad. Sci. Hung. **11**: 81–83.

Jensen, W.A. (*Editor*). 1962. Botanical histochemistry, principles, and practice. Freeman and Co., San Francisco, Calif.

Jones, S.B., and Scott, J.W. 1986. Hypersensitive response in tomato to *Xanthomonas campestris* pv. *vesicatoria*. Plant Dis. **70**: 337–339.

Kartha, K.K., and Gamborg, O.L. 1975. Elimination of cassava mosaïc disease by meristem culture. Phytopathology, **65**: 826–829.

Keen, N.T. 1990. Gene-for-gene complementarity in plant–pathogen interactions. Annu. Rev. Genet. **24**: 447–463.

Klement, Z. 1982. Hypersensitivity. *In* Phytopathogenic prokaryotes. Vol. II. *Edited by* M.S. Mount and G.H. Lacy. Academic Press, Washington, D.C. pp. 149–177.

Knox, J.P., Linstead, P.J., King, J., Cooper, C., and Roberts, K. 1990. Pectin esterification is spatially regulated both within cell walls, and between developing tissues of root apices. Planta, **181**: 512–521.

Kolattukudy, P.E., Kamper, J., Kamper, U., Gonzales-Candelas, L., and Guo, W. 1994. Fungus-induced degradation, and reinforcement of defensive barriers of plants. *In* Host wall alterations by parasitic fungi. *Edited by* O. Petrini and G.B. Ouellette. APS Press, St. Paul, Minn. pp. 67–80.

Lambotte, M., and Perreaux, D. 1979. Histopathology of cassava bacterial blight in susceptible, and tolerant cultivars. *In* Diseases of tropical food crops. *Edited by* H. Maraite and J.A. Meyer. Louvain la Neuve, Belgique. pp. 153–160.

Lemattre, M. 1963. Centre de prolifération, et de nécrose, induits par *Xanthomonas perlargonii* (Brown) Starr, and Burk. dans les tissus de *Pelargonium zonale* : détection, nature, et genèse. C.R.Acad. Sci. Ser. D, **256**: 4494–4497.

Lummerzheim, M., De Olivera, D., Castresana, C., Miguens, F.C., Louzada, E., Roby, D., Van Montagu, M., and Timmermann, B. 1993. Identification of compatible, and incompatible interactions between *Arabidopsis thaliana*, and *Xanthomonas campestris* pv. *campestris*, and characterization of the hypersensitive response. Mol. Plant–Microbe Interact. **6**: 532–544.

Lyon, G.D., and McGill, F.M. 1989. Inhibition of polygalacturonase, and polygalacturonic acid lyase from *Erwinia carotovora* subsp. *carotovora* by phenolics *in vitro*. Potato Res. **32**: 267–274.

Lyon, G.D., Heilbrown, J., Forrest, R.S., and Johnston, D.J. 1992. The biochemical basis of resistance of potato to soft-rot bacteria. Neth. J. Plant Pathol. **92**: 127–133.

Mansfield, J.W. 1983. Antimicrobial compounds. *In* Biochemical plant pathology. *Edited by* C.A. Callow. John Willey & Sons, Chichester. pp. 237–265.

Mbaye, N. 1989. Étude des mécanismes de défense conférant au manioc la résistance aux *Xanthomonas*. Mémoire d'agronome, Université catholique de Louvain, Louvain, Belgium.

Mollenhauer, H.H., and Hopkins, D.L. 1976. Xylem morphology of Pierce's disease-infected grapevines with different levels of tolerance. Physiol. Plant Pathol. **9**: 95–100.

Moreau, M., Catesson, A., Peresse, M., and Czaninski, Y. 1978. Dynamique comparée des réactions cytologiques du xylème de l'oeillet en présence de parasites vasculaires. Phytopathol. Z. **91**: 289–306.

Nicholson, R., and Hammerschmidt, R. 1992. Phenolic compounds, and their role in disease resistance. Annu. Rev. Phytopathol. **30**: 369–389.

Nmasivayam, L., Hedge, R.K., and Balasubramanian, A. 1971. Studies on the biochemical changes in cabbage plants infected with *Xanthomonas campestris* (Pam.) Dow. Phytopathol. Mediterr. **10**: 63–67.

Northcote, D.H., Davey R., and Lay J. 1989. Use of antisera to localize callose, xylan, and arabinogalactan in the cell-plate, primary and secondary walls of plant cells. Planta, **178**: 353–366.

Ouellette, G.B.O., and Rioux, D. 1992. Anatomical, and physiological aspects of resistance to Dutch elm disease. *In* Defense mechanisms of woody plants against fungi. *Edited by* R.A. Blanchette and A. Biggs. Springer Verlag, Berlin. pp. 257–307.

Perreaux, D., Maraite, H., and Meyer, J. 1978*a*. Histopathological study by fluorescent microscopy of cassava stems infected by *Xanthomonas manihotis*. *In* Proceedings of the 4th International Conference on Plant Pathogenic Bacteria. Institut national de la recherche agronomique, Angers, France. pp. 935–941.

Perreaux, D., Terry, E.R., and Persley, G. 1978*b*. Etude des méthodes de criblage pour la résistance du manioc à la bactériose. *In* Cassava bacterial blight. *Edited by* E. R. Terry and G. Persley. Ibadan, Nigeria. pp. 14–17.

Reimers, P.J., and Leach, J.E. 1991. Race-specific resistance to *Xanthomonas oryzae* pv. *oryzae* conferred by bacterial blight resistance gene *Xa-10* in rice (*Oryza sativa*) involves accumulation of a lignin-like substance in host tissues. Physiol. Mol. Plant Pathol. **38**: 39–55.

Rioux, D., Chamberland, H., Simard., M., and Ouellette, G.B. 1995. Suberized tyloses in trees: an ultrastructural, and cytochemical study. Planta, **196**: 125–140.

Rudolph, K. 1993. Infection of the plant by xanthomonads. *In Xanthomonas. Edited by* J.G. Swings, and Civerolo. Chapman and Hall, London, U.K. pp. 193–264.

Teles, F.F.F., Brune, W., Maia, G., Borges, V.E.L., Albuquerque, T.T., Fukuda, C., and Romeiro R.S. 1993. Tuber HCN, and leaf phenols of 16 brazilian cassava (*Manihot esculenta* Crantz) cultivars as related to their resistance to bacterial blight. Rev. Ceres, **40**: 383–389.

Tsuno, K., and Wakimoto, S. 1989. Ultrastructural study on the compatibility between rice leaf vessel system, and various bacteria. *In* Plant pathogenic bacteria. Proceedings of the 7th International Conference of Plant Pathology. *Edited by* Z. Klement, Academia Kiado, Budapest, Hungary. pp. 45–50.

VanderMolen, G.E., Beckman, C.H., and Rodehorst, E. 1977. Vascular gelation: a general response phenomenon following infection. Physiol. Plant Pathol. **11**: 95–100.

VanderMolen, G.E., Beckman, C.H., and Rodehorst, E. 1987. The ultrastructure of tylose formation in resistant banana following inoculation with *Fusarium oxysporum* f.sp. *cubense*. Physiol. Mol. Plant Pathol. **31**: 185–200.

Vasse, J., Frey, P., and Trigalet, A. 1995. Microscopic studies of intercellular infection and protoxylem invasion of tomato roots by *Pseudomonas solanacearum*. Mol. Plant–Microbe Interact. **8**: 241–251.

Wainwright, S.H., and Nelson, P.E. 1972. Histopathology of *Pelargonium* species infected with *Xanthomonas perlargonii*. Phytopathology, **62**: 1337–1347.

Wallis, F.M., and Truter, S.J. 1978. Histology of tomato plants infected with *Pseudomonas solanacearum*, with emphasis on ultrastructure. Physiol. Mol. Pathol. **13**: 307–317.

Wyman, J.G., and Van Etten, H.D. 1978. Antibacterial activity of selected isoflavonoids. Phytopathology, **68**: 583–589.